Bull. Mater. Sci., Vol. 39, No. 4, August 2016, pp. 989–995. © Indian Academy of Sciences.
DOI 10.1007/s12034-016-1251-6

Microwave energy-assisted formation of bioactive CaO–MgO–SiO_2 ternary glass from bio-wastes

ENOBONG R ESSIEN*, VIOLETTE N ATASIE and ESTHER U UDOBANG
Department of Chemical Sciences, Bells University of Technology, P.M.B. 1015 Ota, Nigeria

MS received 8 September 2015; accepted 18 February 2016

Abstract. **Regeneration technique is extensively being sought after as a means of achieving bone repair without adverse immunological response. Silicate-based bioactive glasses containing Mg are gaining increasing attention for their biocompatibility. The current work has been focused on designing a facile and economic route using bio-wastes for synthesizing bioactive glasses in the CaO–MgO–SiO_2 system. Rice husk ash (RHA) obtained from burning rice husk was used as silica source, while Ca was extracted from eggshells for preparing the glass through a modified sol–gel approach. The gel formed was irradiated in microwave before sintering at 950°C for 3 h. Thereafter, bioactivity test was conducted on the samples in simulated body fluid (SBF) at physiological conditions for a maximum of 14 days. Characterization of samples were performed before and after immersion in SBF to evaluate the composition, morphology and phases present in the glass using energy-dispersive X-ray analysis, scanning electron microscopy and X-ray diffraction. Apatite formation was confirmed using Fourier transform infrared spectroscopy. Results obtained showed the presence of diopside, wollastonite and pseudo-wollastonite as major bioactive phases. Hydroxyapatite formed on the material within 3 days in SBF, indicating good bioactivity.**

Keywords. **Rice husk ash; diopside; wollastonite; pseudo-wollastonite; hydroxyapatite.**

1. Introduction

Over the past four decades many promising materials such as glasses, glass–ceramics, ceramics and biopolymers and have been developed to treat complications arising from bone damage. Current bioceramics including Bioglass® 45S5, calcium phosphate-based ceramic materials having mineral composition similar to bone comprising hydroxyapatite ($Ca_{10}(PO_4)_6(OH)_2$, HA), tricalcium phosphate Ca_3PO_4 (TCP), beta-tricalcium phosphate (BCP) and wollastonite ($CaSiO_3$) have excellent bioactivity, which makes them capable of forming direct bonds to host bone when applied *in vivo* [1], thus resulting in regenerative repair of the damaged site [2–5]. Recently, bioactive glasses in the CaO–MgO–SiO_2 system have gained interests in biomedical studies because of evidence suggesting that they possess good bioactivity and cytocompatibility [6–14]. Studies on some bioactive glasses in the CaO–MgO–SiO_2 composition, including calcium silicate, dimagnesium silicate, diopside, akermanite and bredigite, indicate that critical concentration of Ca and Si formed from their dissolution products could stimulate osteoblast proliferation and gene expression [10,12,14–17].

A common observation with CaO–SiO_2–P_2O_5 ternary system glasses when exposed to simulated body fluid (SBF) is that the component CaO–SiO_2 becomes so reactive forming a thick silica gel layer between the apatite layer and the glass [18]. Following the fundamental study of apatite formation in the ternary MgO–CaO–SiO_2 system [19], where MgO partially replaced CaO, MgO was added to CaO–SiO_2-based glass–ceramics to reduce the silica gel layer. Thus, apatite layer having direct contact with the glass substrate formed without the formation of the thick silica gel layer between the apatite and the glass.

Existing methods for preparing CaO–MgO–SiO_2 glasses are through melting method [20,21], and even those utilizing the sol–gel technique prepare Mg-doped glasses with tetraethyl orthosilicate (TEOS) as starting material [22–24]. Melting method requires high temperature processing in the range 1300–1400°C, also TEOS used in the sol-gel processing is expensive. In view of its remarkable bone bonding properties, a cost-effective and facile route for preparing CaO–MgO–SiO_2 glasses is desirable. In the current work, we investigated a cheaper route of preparing highly bioactive MgO–CaO–SiO_2 glass using bio-wastes. Rice husk was used in place of TEOS as silica source and chicken eggshells as precursor for CaO, via a modified sol–gel process. We employed microwave energy irradiation of samples to facilitate drying and enhance surface properties.

2. Materials and methods

2.1 *Materials*

For preparing the glass, SiO_2 was derived from rice husk (Nipede market, Abeokuta, Ogun State, South-west, Nigeria); CaO was extracted from waste chicken eggshells (Ota,

*Author for correspondence (reggiessien@gmail.com)

Ogun State, South-west, Nigeria); MgO was obtained from $Mg(NO_3)_2{\cdot}6H_2O$ (Loba Chemicals), HNO_3 (Riedel-de Haën) and citric acid (Sigma-Aldrich). NaCl, $NaHCO_3$, KCl, $K_2HPO_4{\cdot}3H_2O$, $MgCl_2{\cdot}6H_2O$, $CaCl_2$, trishydroxymethyl aminomethane [Tris-buffer, $(CH_2OH)_3CNH_2$] and HCl reagents were used for preparing SBF solution, all were purchased from Sigma-Aldrich.

2.2 *Preparation of SiO_2 from rice husk*

The rice husk was used as obtained without further treatment. It was burnt in a muffle furnace at 600°C for 6 h to convert it to rice husk ash (RHA).

2.3 *Extraction of Ca from chicken eggshells*

The chicken eggshells were washed with deionized water, oven-dried at 120°C for 2 h, then ball-milled to fine powders. A quantity of 4.4642 g of the powders was dissolved in 5 ml of conc. nitric acid and mixed thoroughly to form a clear solution of $Ca(NO_3)_2$.

2.4 *Synthesis of bioactive glass*

The glass with composition (mol%) $25CaO–25MgO–50SiO_2$ was synthesized by dissolving 99.9 g of citric acid in 180 ml of deionized water using a magnetic stirrer unit. The RHA was added slowly under stirring condition and the mixture was heated at 120°C for 2 h to obtain a clear solution. The stock solution of the eggshells was then added dropwise to the mixture while stirring, followed by the 12.25 g of $Mg(NO_3)_2{\cdot}6H_2O$. The resulting mixture was stirred for 1 h for complete reaction. The obtained sol was kept in an oven at 100°C for 3 h to form a gel followed by drying at 120°C for 24 h. The material was further irradiated in a microwave oven for 15 min to strengthen the gel struts, stabilized at 700°C for 2 h in a muffle furnace to expel nitrates and decompose $Ca(NO_3)_2$ and $Mg(NO_3)_2{\cdot}6H_2O$ to form CaO and MgO, respectively. Samples obtained from the furnace were subjected to ball-milling to obtain powders and then stirred in 98% ethanol to prevent agglomeration. The slurry obtained was dried at 80°C in an oven to expel the ethanol. Samples were finally sintered at 950°C for 3 h for densification.

2.5 *Characterization*

The microstructure of the glass was characterized in EVO/MAIO scanning electron microscope (SEM) equipped with energy-dispersive X-ray analyzer (EDX). The samples were carbon-coated and observed at an accelerating voltage of 15 kV.

Samples were also characterized using X-ray diffraction (XRD) analysis after sintering and after each immersion experiment in SBF to investigate the type of phases present in the glass. The samples were first ground to powder, then 0.1 g of powder was measured in a PANalytical Empyrean X-ray diffractometer using CuKα radiation source of wavelength (λ) = 0.154056 nm operated at 40 kV and 40 mA to obtain the diffraction patterns in the 2θ range from 5° to 90°.

Attenuated total reflectance Fourier transform infrared spectroscopy (FTIR-ATR) (Bruker-Alpha, Platinum ATR) with wavenumber range of 4000–500 cm^{-1} was used to monitor the nature of bonds present in the glass network and to follow the rate of formation of apatite on the surface of the sample for the various days of immersion in SBF.

2.6 *In vitro bioactivity test in SBF*

Assessment of bone bonding ability was performed using the standard *in vitro* procedure [25]. The acellular SBF was prepared using analytical grade reagents; NaCl, $NaHCO_3$, KCl, $K_2HPO_4{\cdot}3H_2O$, $MgCl_2{\cdot}6H_2O$, $CaCl_2$, trishydroxymethyl aminomethane [Tris-buffer, $(CH_2OH)_3CNH_2$] and 1 M HCl with ions concentration shown in table 1. Samples were immersed in the SBF solution at a concentration of 0.01 g ml^{-1} in clean sterilized plastic bottles, which were initially washed using HCl and deionized water. The bottles were placed inside a thermostated incubator at a temperature of 36.5°C at an initial pH of 7.3. The SBF solutions were not refreshed throughout the period of immersion to allow for pH monitoring of the solution daily for 14 days using a pH meter (Hanna, HI96107). The samples once extracted from the SBF solution after given days of 3, 7 and 14 were rinsed with deionized water and left to dry at ambient temperature in a desiccator. Formation of apatite layer on the glass surface was evaluated by SEM, XRD and FTIR.

3. Results and discussion

3.1 *Gelation of the RHA and formation of glass*

RHA contains high percentage of SiO_2 required to serve as network former for the glass, but is insoluble in water under ambient conditions. To form the sol, the RHA was reacted with citric acid ($C_6H_8O_7$) solution to give a four-fold coordination complex (scheme 1). Having formed the carboxyl (COOH) groups of the resulting complex imparted solubility

Table 1. Ion concentrations (mM) in human plasma in comparison with SBF.

Ion	Na^+	K^+	Mg^{2+}	Ca^{2+}	Cl^-	HCO_3^-	HPO_4^{2-}	SO_4^{2-}
SBF	142.0	5.0	1.5	2.5	147.8	4.2	1.0	0.5
Human plasma	142.0	5.0	1.5	2.5	103.0	27.0	1.0	0.5

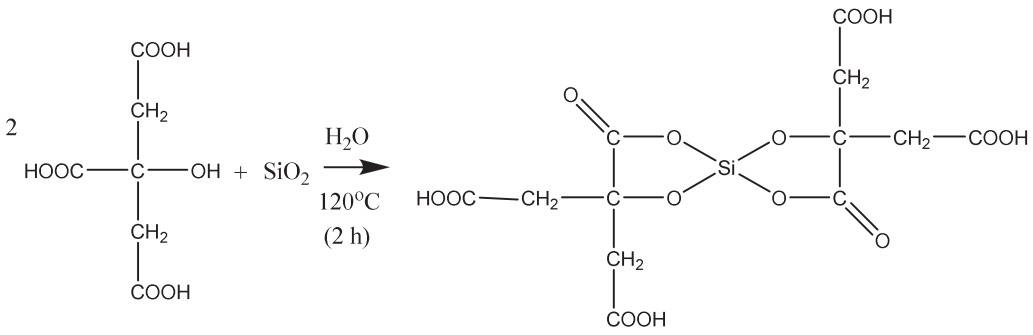

Scheme 1. Network structure showing linkage between citric acid and siloxane groups from RHA.

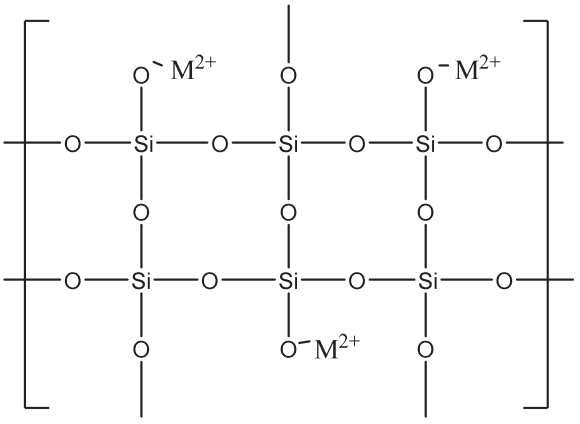

Scheme 2. Polymeric structure of the glass after heating at 950°C for 3 h showing siloxane bonds disrupted by network modifier ions M^{2+} ($M^{2+} = Ca^{2+}$ or Mg^{2+}).

resulting in the formation of a sol. The addition of network modifier ions of Ca^{2+} and Mg^{2+} and further reactions led to polymerization of the complex to form a gel. During the drying stages, the 3D modified silicate network contracts and becomes rigid as water present in the pores are expelled [26]. During calcinations the citric acid moiety is burnt off giving rise to the glass with network structure having some of the bonding oxygens (BO's) of the siloxane bonds disrupted by Ca^{2+} and Mg^{2+} ions to form reactive non-bonding oxygen bonds (NBO's) as represented in scheme 2.

3.2 *Composition of glass*

The EDX spectrum of the glass (figure 1) confirms the composition of the glass to be (mol%) 25CaO–25MgO–50SiO_2 as prepared. The $CaCO_3$ present in the eggshells reacted with the HNO_3 to form soluble $Ca(NO_3)_2$ (eq. 1), which was added to the glass and sintered to yield CaO.

$$CaCO_3 + 2HNO_3 \rightarrow Ca(NO_3)_2 + CO_2 + H_2O \qquad (1)$$

It can be inferred from the EDX result that both the rice husk and chicken eggshells contain high percentage of SiO_2 and CaO, respectively. The small peaks of Na and K observed in the spectrum are present as impurities, introduced from the rice husk source. There is no carbon peak observed in the material, indicating that the sintering temperature of 950°C for 3 h was adequate to completely eliminate residual organics emanating from RHA and citric acid.

3.3 *Morphology*

Figure 2 shows the SEM micrographs of the glass before and after incubation in SBF. As observed in figure 2a, after sintering at 950°C for 3 h, the glass presents a microstructure with sparsely distributed glass particles, most of which form clusters along with some voids.

It is also observed from the micrograph that the glass particles are well dispersed, which is attributed to the efficiency of the modified sol–gel technique and drying procedures adopted in this work. The average particle size of the glass as determined from the micrograph was 4 μm. Such microstructures are important for cell adhesion [27]. After immersion in SBF for 3 days, particle density increases on the surface of the glass due to the formation of HA, figure 2b. As immersion days increased to 7, apatite colony increased, forming well-distributed particles on the surface of the glass as shown in figure 2c. After 14 days in SBF, the glass surface became almost completely covered with thick apatite layers [28] (figure 2d).

3.4 *Diffraction patterns*

The XRD spectra showing the diffraction patterns and phases present are represented in figure 3. The parent glass (figure 3a) shows the presence of different phases. The phases identified are wollastonite [29], pseudo-wollastonite [30], diopside [30], calcite [31] and cristobalite [32]. Previous reports [20–25] show that glasses containing wollastonite and diopside possess good bioactive potentials.

The glass presented a semi-crystalline structure judging from the intensity of the peaks and their diffusive nature at the baseline. This is due to short-range ordering of the material during sintering at 950°C for 3 h, which was not sufficient to cause full crystallization of the material. Complete crystallinity decreases apatite-forming kinetics on a glass surface [33]. Hence the semi-crystalline properties exhibited by the glass is expected to increase dissolution rates and bioactivity in biological fluids [33] based on the well-known bone-bonding mechanisms of bioactive glasses, which were first proposed by Hench and Wilson [34]. In the sequence of interfacial reactions on the surface of Bioglass® in contact with body fluids, the bioactive glass first dissolves to form a silica-gel layer. Later, an amorphous calcium phosphate forms from the hydrated silica-gel, and finally, apatite

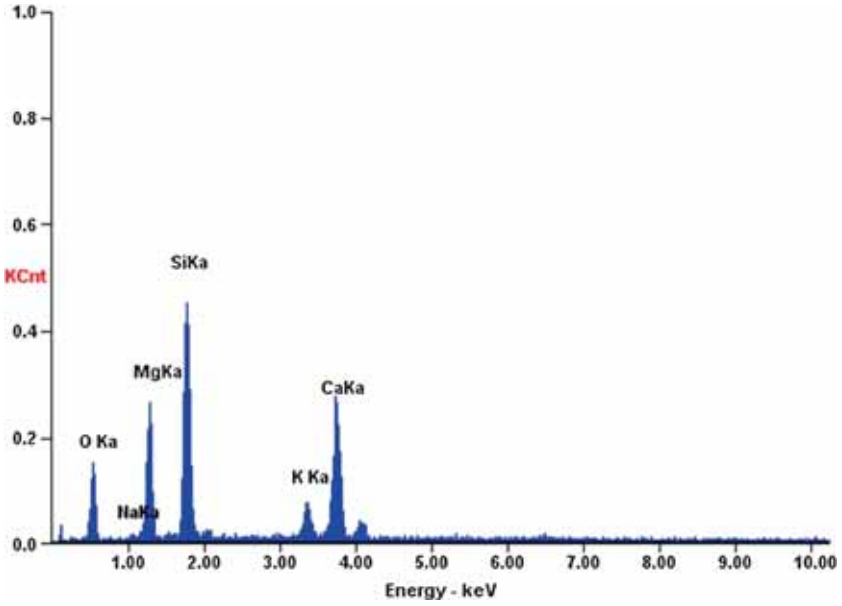

Figure 1. EDX spectrum showing the composition of the glass after sintering at 950°C for 3 h.

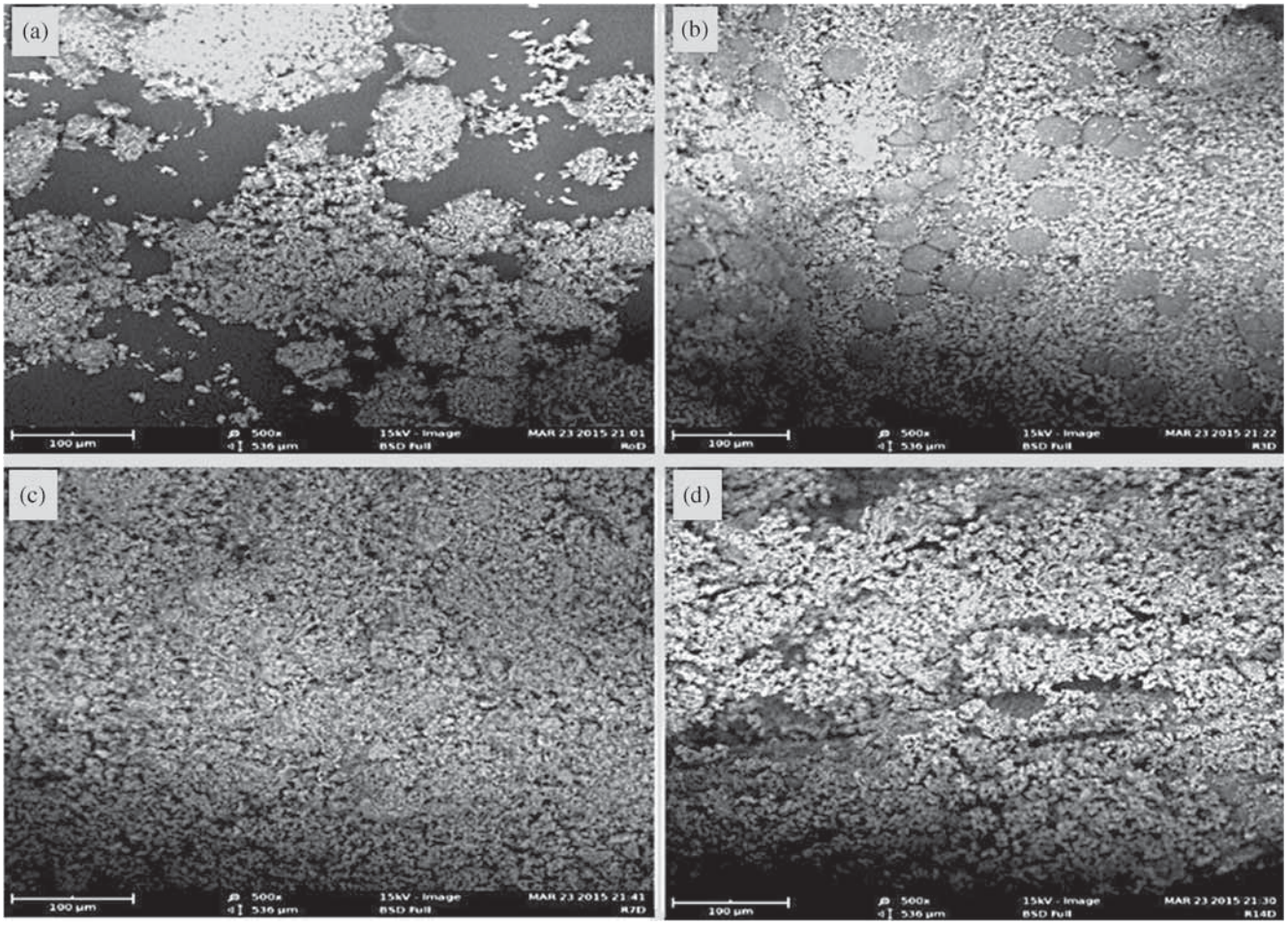

Figure 2. SEM micrographs depicting the glass microstructure (**a**) after sintering at 950°C, and (**b**, **c** and **d**) after immersion in SBF for 3, 7 and 14 days, respectively, showing growth of apatite. All images are with the same magnification.

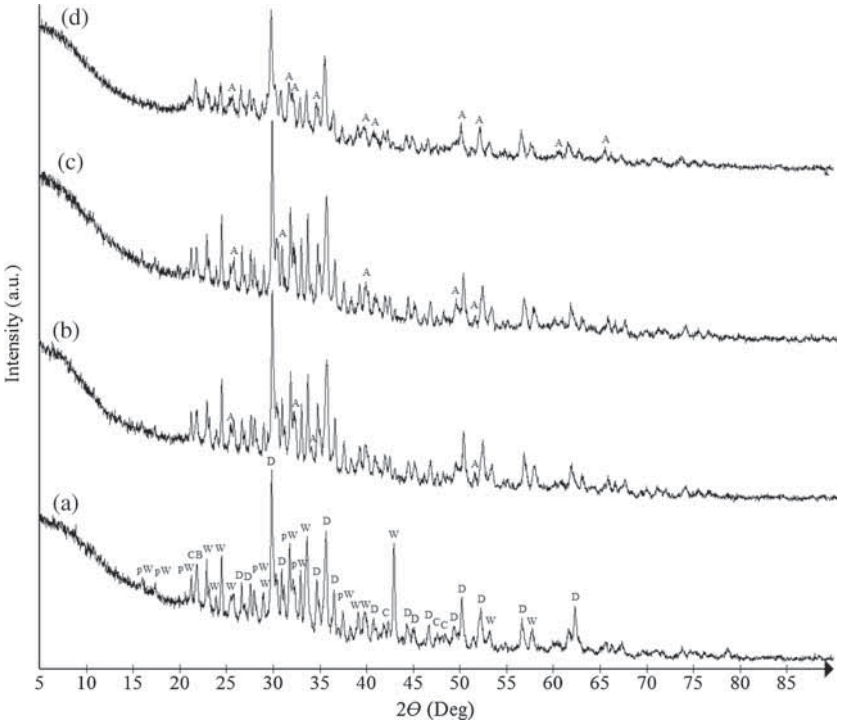

Figure 3. X-ray diffraction patterns of the (**a**) glass as sintered, after immersion in SBF for a period of (**b**) 3, (**c**) 7 and (**d**) 14 days (W, wollastonite; pW, pseudo-wollastonite; CB, cristobalite; D, diopside; C, calcite; A, hydroxyapatite).

crystallites nucleate and grow from the amorphous calcium phosphate. This sequence of reactions can be followed with FTIR [35,36].

After immersion for 3 days, figure 3b, new peaks emerge which were identified as HA according to the standard PDF file JCPDS No. 9-0432 [37]. With increased immersion time to 7 and 14 days, figure 3c and d, respectively, more apatite peaks are observed in the spectra, which matched the standard PDF file JCPDS No. 9-0432 in intensity and angular location. There is a significant change in diffraction pattern of the glass after 14 days in SBF. The intensity of most of the major peaks decreased, indicating that the material has biodegradable properties [10,14].

3.5 *Reactivity of glass in SBF*

The pH changes of the glass in SBF for 14 days are depicted in figure 4. During the first 3 days, steep rise in pH was observed. This is attributed to ion exchange occurring between the Ca^{2+} and Mg^{2+} ions on the surface of the glass and H^+ or H_3O^+ ions of the SBF solution, which satisfies stage 1 of reactions of bioactive glasses in physiological fluids [38]. After the 3rd day, the pH rises slowly until day 8. This signifies the re-adsorption of Ca^{2+} from the SBF solution unto the glass surface to form HA [39], thus slowing down the ion release rate on the glass surface. The pH remains unchanged from the 8 to 11th day as more re-adsorption of Ca^{2+} occurs between the SBF solution and the glass surface, but increases slightly to a saturated value of 9.9 between 12

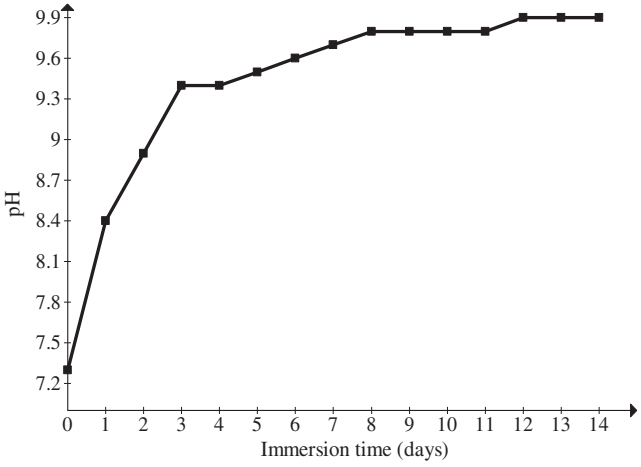

Figure 4. pH changes of the glass in SBF solution for a maximum of 14 days.

and 14 days, indicating that apatite-forming kinetics is complete. The steep rise in pH during the first 3 days from 7.3 to 9.4 and culminating in a pH value of 9.9 after 14 days of immersion in SBF indicates that the glass has a high rate of reactivity and therefore resorption in physiological fluids. This feature is one of the basic requirements of a material to be used as scaffold for guiding cell formation and proliferation [40].

The high reactivity of the glass in SBF can be attributed to the enhanced surface topography of the glass. After 14 days

in SBF, the glass begins to degrade releasing ionic dissolution products, such as soluble silica and calcium ions, which cause the pH of the solution to rise to 9.9. These ions when present in critical concentrations could be biologically active [28]. Recent studies have shown that bioactive resorbable glasses and their ionic dissolution products enhance osteogenesis by regulating osteoblast proliferation, differentiation and gene expression [15,40–42]. In the presence of critical concentrations of Si and Ca ions, within 48 h, osteoblasts that are capable of differentiating into a mature osteocyte phenotype begin to proliferate and regenerate new bone [40].

3.6 *FTIR assessment of bonds and confirmation of apatite*

The FTIR spectra of the samples before and after exposure to SBF for 3, 7 and 14 days are shown in figure 5. Before the tests the sample exhibited a spectrum characterized by peaks at 1479, 985, 875, 602 and 506 cm^{-1}. The band around 1479 cm^{-1} is due to the presence of ionic surface carbonates [43] in the sample caused by adsorption of atmospheric CO_2 during the sol preparation by labile surfaces formed by the alkaline earth metal cations Ca^{2+} and Mg^{2+}. The small peak at 985 cm^{-1} corresponds to Si–O–Si(s, asym) asymmetric stretching mode [44], while the sharp peak at 875 cm^{-1} is related to ($Si–O^-$) of SiO_4^{4-} tetrahedra having two non-bonding oxygen per tetrahedron (Si–O–2NBO) [44], formed from the presence of network-modifying cations Ca^{2+} and Mg^{2+}. Also, the one at 506 cm^{-1} signifies the bending vibrational mode of Si–O–Si bond. The small peak observed around 602 cm^{-1} is related to the presence of crystalline phase in the sample [45] as indicated by the XRD result figure 3a. After 3 days in SBF, the peak at 985 cm^{-1} increased in intensity as exchange of ions occurs between the glass surface and the solution (stage 1) [38], signalling the onset of formation of hydrated SiO_2^- gel layer [2,46].

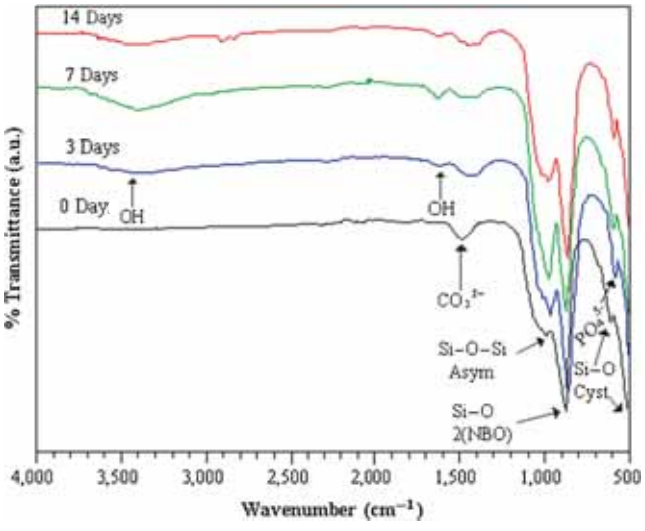

Figure 5. FTIR spectra of the glass before immersion in SBF and after immersion for 3, 7 and 14 days, showing the formation of apatite bonds.

This suggestion is supported by the appearance of a broad OH band centred at 3380 cm^{-1} and another weak band at 1637 cm^{-1}, resulting from water absorption. Furthermore, the peak near 602 cm^{-1} intensifies indicating the formation of calcium phosphate layer due to uptake of P from the solution [45]. The hydrated SiO_2 gel layer becomes enriched after 7 days in SBF, as shown in the spectra in figure 5, by the lengthening of the peak at 985 cm^{-1} and increase in intensity of the water absorption bands near 3380 and 1637 cm^{-1}. As the calcium phosphate layer turns crystalline after 14 days, the carbonate band at 1479 cm^{-1} develops two small modes, while the phosphate peak around 602 cm^{-1} becomes more intense and sharper, characteristic of crystalline apatite [47]. At this time, the hydrated SiO_2-rich layer and the water absorption bands reduced considerably in intensity, suggesting that apatite layer has covered the surface of the glass to a large extent [46,48], and thus confirming the XRD result presented in figure 3d.

4. Conclusion

A CaO–MgO–SiO_2 semi-crystalline bioactive glass has been successfully formed from two bio-waste materials, rice husk and chicken eggshells, as rich sources of SiO_2 and CaO, respectively. Results showed that there was absence of agglomeration of glass particles and consequently, good surface area important for reaction of the glass in body fluid. This was evident in the rapid pH changes during the period of immersion in SBF and formation of apatite within 3 days. We therefore conclude that our synthesis procedure is facile and economical and may be applied in the preparation of ternary system of CaO–MgO–SiO_2 bioactive glasses for bone repair.

Acknowledgement

We are thankful to Mr. Femi Igbari, College of NanoScience and Technology, Soochow University, China, for his assistance with the EDX and XRD characterization as well as Mr. Isa Yakubu, Ahmadu Bello University, Zaria, for the SEM analysis.

References

[1] Oliveira J M, Correia R N and Fernandes M H 1995 *Biomaterials* **16** 849

[2] Hench L L 1998 *J. Am. Ceram. Soc.* **81** 1705

[3] Nonami T and Tsutsumi S J 1999 *Mater. Sci. Mater. Med.* **10** 475

[4] Siriphannon P, Hayashi S, Yasumori A and Okada K 1999 *J. Mater. Res.* **14** 529

[5] Wu C T, Chang J, Wang J Y, Ni S Y and Zhai W Y 2005 *Biomaterials* **26** 2925

[6] Siriphannon C P, Kameshima Y, Yasymori A, Okada K and Hayashi S 2002 *J. Eur. Ceram. Soc.* **22** 511

[7] Liu X Y, Ding C X and Chu P K 2004 *Biomaterials* **25** 1755

[8] Liu X Y, Morra M, Carpi A and Li B E 2008 *Biomed. Pharmacother.* **62** 526

[9] Gou Z R, Chang J, Zhai W Y and Wang J Y 2005 *J. Biomed. Mater. Res.* **B73** 244

[10] Wu C T and Chang J 2007 *J. Biomed. Mater. Res.* **B83** 153

[11] Chen X C, Ou J, Kang Y Q, Huang Z B, Zhu H Y, Yin G F and Wen H M 2008 *J. Mater. Sci.: Mater. Med.* **19** 1257

[12] Chen X C, Liao X M, Huang Z B, You P L, Chen C, Kang Y Q and Yin G F 2010 *J. Biomed. Mater. Res.* **B93** 194

[13] Ou J, Kang Y Q, Huang Z B, Chen X C, Wu J, Xiao R C and Yin G F 2008 *Biomed. Mater.* **3** 015015

[14] Ni S Y and Chang J 2009 *J. Biomed. Appl.* **24** 139

[15] Xynos I D, Edgar A J, Buttery L D, Hench L L and Polak J M 2001 *J. Biomed. Mater. Res.* **55** 151

[16] Gough J E, Notigher I and Hench L L 2004 *J. Biomed. Mater. Res.* **A68** 640

[17] Valerio P, Pereira M M, Goes A M and Leite M F 2004 *Biomaterials* **25** 2941

[18] Ohtsuki C, Kokubo T, Takatsuka K and Yamamuro T 1991 *J. Ceram. Soc. Jpn.* **99** 1

[19] Tsuru K, Ohtsuki C and Osaka A 1995 *Effect of MgO and BaO on bioactivity of CaO-SiO_2 glasses*. In Proc. XVII Int. Cong. on Glass G Fangtian (ed) (Beijing, China: Chinese Ceramic Society) vol 5 p 85

[20] Cannillo V, Pierli F, Sampath S and Siligardi C 2009 *J. Eur. Ceram. Soc.* **29** 611

[21] Sainz M A, Pena P, Serena S and Caballero A 2010 *Acta Biomater.* **6** 2797

[22] Arstila H, Hupa L, Karlsson K H and Hupa M 2008 *J. Non-Cryst. Solids* **354** 722

[23] Ma J, Chen C Z, Wang D G and Hu J H 2011 *Ceram. Int.* **37** 1637

[24] Fooladi A A I, Hosseini H M, Hafezi F, Hosseinnejad F and Nourani M R 2013 *J. Biomed. Mater. Res.* **A101** 1586

[25] Kokubo T and Takadama H 2006 *Biomaterials* **27** 2907

[26] Hwang S-W, Kim T-Y and Hyun S-H 2010 *Microporous Mesoporous Mater.* **130** 295

[27] Yamasaki Y, Yoshida Y, Okazaki M, Shimazu A, Uchida T and Kubo T 2002 *J. Biomed. Mater. Res.* **62** 99

[28] Hench L L 2006 *J. Mater. Sci. Mater. Med.* **17** 967

[29] Barkley M M, Downs R T and Yang H 2011 *Amer. Miner.* **96** 797

[30] Richet P, Mysen B and Ingrin J 1998 *Phys. Chem. Mater.* **25** 401

[31] Liu X, Lu X, Liu X and Zhou H 2015 *Amer. Miner.* **100** 172

[32] Lin K S K, Yao-Hung T, Mou Y, Yu-Chuan H, China-Min Y and Chan J C C 2005 *Chem. Mater.* **17** 4493

[33] Matsui M, Sato T and Funamori N 2014 *Amer. Miner.* **99** 184

[34] Hench L L and Wilson J 1984 *Science* **226** 630

[35] Clark A E and Hench L L 1989 *Non-Cryst. Solids* **113** 195

[36] La Torre G and Hench L L 1993 *Analysis of bioactive glass interfacial reactions using Fourier-transform infrared reflection spectroscopy.* In handbook on characterization techniques for the solid-solution interface J H Adair, J A Casey and S Venigalla (eds) (Westerville, OH, USA: American Ceramic Society) p 117

[37] Boccaccini A R, Chen Q, Lefebvre L and Gremillard L 2007 *Faraday Discuss.* **136** 27

[38] Chen Q Z, Thompson I D and Boccaccini A R 2006 *Biomaterials* **27** 2414

[39] Mourino V and Boccaccini A R 2010 *J. Royal Soc. Interface* **7** 209

[40] Xynos I D, Hukkanen M V J, Batten J J, Buttery L D, Hench L L and Polak J M 2000 *Calcif. Tissue Int.* **67** 321

[41] Hench L L 2009 *J. Eur. Ceram. Soc.* **29** 1257

[42] Hench L L, Xynos I D, Edgar A J, Buttery L D K, Polak J M, Zhong J P, Liu X Y and Chang J 2002 *J. Inorg. Mater.* **17** 897

[43] Cerruti M and Morterra C 2004 *Langmuir* **20** 6382

[44] Aina V, Malavasi G, Fiorio Pla A, Munaron L and Morterra C 2009 *Acta Biomater.* **5** 1211

[45] Chen Q-Z, Yuan L Y, Jin L-Y, Quinn J M W and Komesaroff P A 2010 *Acta Biomater.* **6** 4143

[46] Peitl O, Zanotto E D and Hench L L 2001 *J. Non-Cryst. Solids* **292** 115

[47] Oliveira J M, Correia R N and Fernandes M H 2002 *Biomaterials* **23** 371

[48] Filho O P, LaTorre G P and Hench L L 1996 *J. Biomed. Mater. Res.* **30** 509